An Intelligent Anti-Islanding Scheme for Synchronous-Based Distributed Generation Using Reduced-Noise Morphological Gradient

S. Shadpey* and M. Sarlak*(C.A.)

Abstract: This paper presents a pattern recognition-based scheme for detection of islanding conditions in synchronous- based distributed generation (DG) systems. The main idea behind the proposed scheme is the use of spatial features of system parameters such as the frequency, magnitude of positive sequence voltage, etc. In this study, the system parameters sampled at the point of common coupling (PCC) were analyzed using reduced-noise morphological gradient (RNMG) tool, first. Then, the spatial features of the RNMG magnitudes were calculated. Next, to optimize and increase the ability of the proposed scheme for islanding detection, the best features with a much discriminating power were selected based on separability index (SI) calculation. Finally, to distinguish the islanding conditions from the other normal operation conditions, a support vector machine (SVM) classifier was trained based on the selected features. To investigate the power of the proposed scheme for islanding detection, the results of examinations on the various islanding conditions including system loading and grid operating state were presented. These results show that the proposed algorithm reliably detect the islanding condition within 32.7 ms.

1 Introduction

IN distribution systems throughout the world, the use of DG is increasing because of its potential for providing reliable service at a lower price for customers. The integration of DGs in the distribution system poses serious conditions, which need to be addressed [1]. The unintentional islanding is one of these conditions in which a distribution system –because of line faults, equipment failures, and human errors– is electrically separated from the remainder of the power system, and fed by DGs connected to it [2].

Because of the uncontrolled operation of islanding, the allowable limits of voltage, frequency, and power quality indices may be violated. In addition, the unintentional islanding is hazardous for the public and utility workers. Thus, the islanded system should be immediately de-energized after islanding detection. IEEE std.1547 [3] emphasizes on maximum delay of 2 sec for detecting islanding and disconnecting all DGs from the distribution system.

The main philosophy of islanding detection is to analyze the measured system parameters such as frequency, voltage, and active and reactive powers at the point of common coupling (PCC) and/or to monitor the states of circuit breakers throughout the distribution system. Up to now, extensive research has been conducted resulting in many schemes for anti-islanding protection. Islanding detection methods can be mainly classified as communication and non-communication-based techniques. The former methods are required to receive data from, at least, one bus of the distribution system other than the local bus. In contrast, the latter methods need only local bus data for decision making whether the islanding condition has been occurred or

not.

The communication-based methods [4-5] have a small non-detection zone (NDZ) without any negative effect on power quality. However, for installation of these methods, the telecommunication infrastructure should be provided which needs too much investment. In addition, the performance of such methods highly depends on the reliability of the communication systems. Therefore, for the detection of the islanding condition in a reliable way, the methods are replaced by non-communication-based methods and/or combined with them.

The non-communication-based methods can be categorized as passive and active methods. The latter methods are based on analyzing the measured system parameters at the PCC after injecting a small disturbance into the DG output. Having a small NDZ is the advantage of the active methods [6-9] and [33, 34]. However, the power quality indices may be deteriorated by these methods during normal conditions.

On the other hand, the passive methods [10-20], [31, 32], and [35-37], which detect islanding condition by continuous monitoring of the system parameters such as frequency, voltage, and active and reactive powers at the PCC, suffer from a large NDZ. To decrease the NDZ, the islanding detection has been considered as a pattern recognition problem. For a pattern recognition-based islanding detection, the very important steps are extraction and selection of the most valuable features of the measured system parameters. Feature extraction and selection steps can be performed using the suitable signal processing methods and an appropriate index, respectively.

Up to now, the pattern recognition-based islanding detection methods mostly rely on extracting hidden features of the measured and estimated system parameters using advanced digital filters characterized by more computational burden and complexity. Moreover, this category of islanding detection methods suffers from the noises which practically exist in the environment. The most important digital filters used in these anti-islanding schemes are: discrete wavelet transform (DWT) [10], s-transform (ST) [12], hyperbolic s-transform (HST) [11], t-transform (TT) [11], tt-transform (TTT) [11] and duffing oscillations [18]. In [13], the authors used a simple digital filter based on the basic mathematical morphology (MM) to propose a novel method for fault detection and faulty phase selection in an islanded distribution system. In other words, the authors have not proposed a separate technique to detect an islanding situation.

In this paper, a non-communication-based intelligent islanding detection scheme is proposed which is based on an effective simple digital filter being robust to the environmental noises. It is called reduced-noise morphological gradient (RNMG) [21, 22] whose characteristic is in highlighting the points of the signal

with an irregularity. To improve the performance of the proposed scheme, the separability index (SI) [23]-[24] has been used to select the most valuable features. Also, it is noticeable that the support vector machine (SVM) classifier [25] is used in the proposed scheme as a decision-maker for islanding detection. The proposed scheme is capable of islanding detection in synchronous-based distributed generation systems in situations with the least exchanged power between the DG resources and the distribution system.

The rest of the paper is organized as follows. The theoretical basis of the proposed scheme including the RNMG technique, the SI measure, and the SVM classifier are presented in Section 2. The proposed scheme framework is presented in Section 3. In Section 4, Modeling of a typical distribution system, data generation, and feature extraction/selection and classifier algorithm are explained. Then, in Section 5, the simulation results are given and discussed. In the end, the conclusion is given.

2 Theoretical Review

In this section, the theoretical basis behind the proposed scheme is presented.

2.1 Reduce-Noise Morphological Gradient (RNMG)

The theory of mathematical morphology (MM) is based on set theory, integral geometry, and lattice algebra. This tool is very powerful for extracting time features of a signal [21, 22]. The fundamental MM-based operations are dilation and erosion. These operations are characterized as the basic words in morphological literature and defined by (1) and (2), respectively [21, 22].

$$f \oplus B = \max_s \left\{ f(x+s) + B(s) \mid (x+s) \in D_f, s \in D_B \right\} \quad (1)$$

$$f \ominus B = \min_s \left\{ f(x+s) - B(s) \mid (x+s) \in D_f, s \in D_B \right\} \quad (2)$$

where f and D_f are the signal under processing and its domain, respectively. Besides, B and D_B are the structuring element (SE) and its domain, respectively. An SE is conceptually similar to the data window. The dilation applies expansion process and the erosion applies shrinking process for the input signal. They show the difference between a processed signal and the original signal.

By combining the dilation and erosion operations, the opening and closing filters which change the geometry features of signals are constructed. They are defined [22] respectively by

$$f \circ B = (f \ominus B) \oplus B \quad (3)$$

$$f \bullet B = (f \oplus B) \ominus B \quad (4)$$

The geometry attributes of signals are changed using the opening and closing filters. The former filter

expands the shrunken signal and the latter filter shrinks the expanded one. The required calculations in these filters only include addition, subtraction, maximum and minimum operations. They show the convex and concave features of the signal. However, these filters do not show all the features of the signal under processing.

The morphology gradient (MG) aims at extracting the signal gradient which is a powerful tool for detecting signal irregularities. Mathematically, this gradient is the difference between expanding and shrinking of a signal and is defined [22] by

$$\delta_{MG}(f) = (f \oplus B) - (f \ominus B) \tag{5}$$

In fact, the MG effectively depresses the steady-state components and increases the transient ones of the signal. However, this form of MG has an unacceptable sensitivity to environmental noises. Hence, the RNMG filter [21] is used which is more immune than the MG to the environmental noises. It is defined by

$$\delta_{RNMG}(f) = (A \bullet B) \oplus B - A \bullet B \tag{6}$$

where A is the opening-closing operation that is applied to filter the noises. It smooths the signal by first closing and then dilation and is defined by

$$A = (f \bullet B) \circ B \tag{7}$$

According to (6), the perfect signal edge will be extracted based on the arithmetic difference between the processed signal by the above process and the signal before dilation.

2.2 Separability Index

In the pattern recognition literature, a feature with a little discriminating power in feature space is determined as a "weak feature". If a set of weak features is selected, the constructed pattern recognition system may have no acceptable performance. In other words, the selection of effective features would result in a more simple and accurate system. In this paper, to determine the strong features, the separability measure presented in [23, 24] was used. The larger the measure, the more effective a feature. This measure is given by

$$J = \frac{trace\{S_b\}}{trace\{S_w\}} \tag{8}$$

where J is separability measure and S_w and S_b are the within-class and between-class scatter matrices, respectively [23, 24]. The former matrix for M classes is given by

$$S_W = \sum_{i=1}^{M} P_i S_i \tag{9}$$

where

$$S_i = E\left[(X - \mu_i)(X - \mu_i)^T\right] \tag{10}$$

$$P_i = \frac{n_i}{N} \tag{11}$$

where S_i is the covariance matrix of the i-th class, P_i is the a-priory probability of the i-th class, $X = [x_1, x_2, \ldots, x_m]$ is an m-dimensional feature vector, n_i is the number of samples belong to the i-th class out of the total number of samples, N, and μ_i is the mean vector of the pattern vectors belong to the i-th class. Also, the between-class scatter matrix (S_b) for M classes is given by

$$S_b = \sum_{i=1}^{M} P_i (\mu_i - \mu_0)(\mu_i - \mu_0)^T \tag{12}$$

where

$$\mu_0 = \sum_{i=1}^{M} P_i \mu_i \tag{13}$$

where μ_0 is the global mean vector. When the samples in the feature space are well clustered around their mean and the clusters of different classes are well separated, the magnitude of J, as defined by (8), is large.

2.3 SVM Classifier

Originally, the SVM algorithm is formulated to solve binary classifications [25]. In order to reach an optimal solution, it nonlinearly maps the feature vectors from a low dimensional space onto a higher dimensional space first, in which the classes are more linear separable than the former. Then, an optimal hyperplane as a linear decision function is obtained to achieve the maximum margin between the data in two classes. Unfortunately, the optimal hyperplane calculation requires the dot product of feature vectors which specifically causes a high computational burden in a higher-dimensional space. Therefore, to reduce the computational burden, the dot product in the higher dimensional feature space is calculated in the lower dimensional feature space using kernel functions [25].

Mathematically, the optimal hyperplane determination can be stated as an optimization problem. Given the data including feature vector-label pairs (t_i, y_i), $i = 1, \ldots, l$ where $t_i \in \Re^n$, l the whole number of sample vectors and $y_i \in \{-1, 1\}$, the hyperplane having the largest margin between two classes is obtained by providing a solution for the following optimization problem:

$$\text{max: } \tau(\mathbf{\alpha}) = \sum_{i=1}^{l} \alpha_i$$
$$- \frac{1}{2} \sum_{i=1}^{l} \sum_{j=1}^{l} \alpha_i \alpha_j y_i y_j K(t_i, t_j) \tag{14}$$

$$\text{s.t: } \sum_{i=1}^{l} \alpha_i y_i = 0 \ , \ 0 \le \alpha_i \le C \tag{15}$$

where α_i, $i = 1, …, l$ are the Lagrange multipliers of the feature vectors and C is a penalty factor which controls the tradeoff between separation margin and training errors. Also, K is the kernel function.

An interesting point of the solution of the optimization problem is that the Lagrange multipliers of the closest feature vectors of two classes are only nonzero. These feature vectors are called "support vectors" (SVs), and the optimal hyperplane is constructed based on them. In other words, to judge the class label of any unlabeled feature vector $\mathbf{z}$, the following decision function is applied:

$$f(\mathbf{z}) = sign\left(\sum_{j=1}^{n_s} \alpha_{k_j} y_{k_j} K\left(t_{k_j}, z\right) + b\right)$$
$$= \begin{cases} +1 \Rightarrow y_z = +1 \\ -1 \Rightarrow y_z = -1 \end{cases} \quad (16)$$

where $\mathbf{z}$, n_s, α_k, and y_k are unlabeled feature vector, the number, the Lagrange multipliers, and class labels of SVs, respectively. Moreover, b is the offset term calculated according to the following equation by substituting one of the SVs only in (16):

$$b = \begin{cases} 1 - \sum_{j=1}^{n_s} \alpha_{t_j} y_{t_j} K\left(\mathbf{x}_{t_j}, \mathbf{x}_{t_k}\right) & \text{if } y_{t_k} = 1 \\ -1 - \sum_{j=1}^{n_s} \alpha_{t_j} y_{t_j} K\left(\mathbf{x}_{t_j}, \mathbf{x}_{t_k}\right) & \text{if } y_{t_k} = -1 \end{cases} \quad (17)$$

Many kernel functions such as polynomial, Multi-layer perception (MLP), linear and Radial Basis Function (RBF) are used by the SVM [25]:

• Polynomial kernel function with degree d is given as

$$K(\mathbf{x}, u) = \left(\mathbf{x}^T u + 1\right)^d \quad (18)$$

• Multi-layer perception (MLP) kernel function is given as

$$K(\mathbf{x}, u) = \tanh\left(\kappa \mathbf{x}^T u + 1\right), \quad \kappa > 0 \quad (19)$$

• Linear kernel function is given as

$$K(\mathbf{x}, u) = \mathbf{x}^T u. \quad (20)$$

• Radial Basis Function (RBF) kernel function is given as

$$K(\mathbf{x}, u) = \exp\left(-\gamma \|\mathbf{x} - u\|^2\right), \quad \gamma > 0 \quad (21)$$

where $\mathbf{x}$ is the training data vectors and u is the testing data vectors, and d, κ, and γ are magic parameters that should be chosen using a model selection method such as k-fold cross-validation [27].

3 Proposed Scheme Framework

The flowchart of the proposed scheme framework for islanding detection is shown in Fig. 1.
The scheme units are:
1) Signal acquisition, in which the current and voltage signals are sampled.
2) Selected features calculation, in which the predefined features are calculated according to the RNMG filter and SI.
3) Pre-processing, which is performed to avoid any numerical instability, and is accomplished through the feature normalization.
4) Classification, whose output determines whether islanding has occurred or not.
5) Remedial action, which is the disconnection of the DG from the distribution system and de-energizing of DG.

4 Case Study

4.1 System Modeling

In order to demonstrate the ability of the proposed scheme for islanding detection, we considered the typical system in [26]. Fig. 2 shows the system in which there are two 10 MVA synchronous-based DGs and 4 loads including L1, L2, L3, and L4. In addition, the short circuit level of the sub-transmission is 1000 MVA. The reader can get more details of the system in the appendix at the end of the paper. The authors simulated the system in PSCAD/EMTDC software environment. It is worth noting that the authors used single mass models of the DGs in simulations. Besides, they simulated the transmission lines, considering the frequency-dependent parameter model.
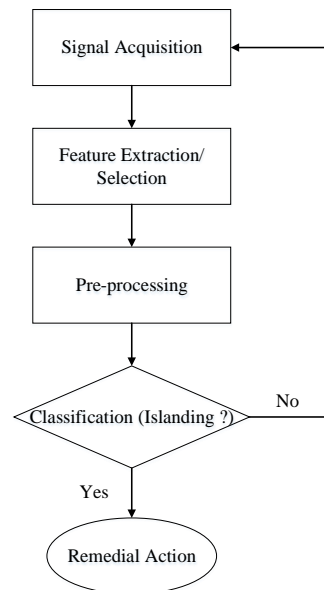

Fig. 1 Flowchart of the proposed scheme framework for islanding detection.
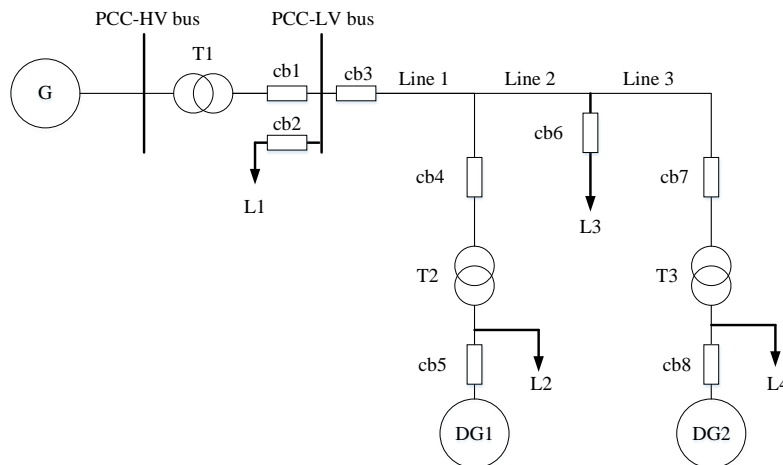
Fig. 2 Typical system. Symbols are: G (grid), HV (high voltage), LV (low voltage), T (power transformer), L (load) and DG (synchronous distributed generation), cb (circuit breaker) [26].

Table 1 Various events of islanding and non-islanding conditions.

Scenario	Event description	Number of Cases
Islanding	1. Opening of cb1 for the condition of islanding of DGs with the LV bus load.	9
	2. Opening of cb3 for the condition of islanding of DGs without the LV bus load.	9
	3. Three-phase fault on the HV bus (for one cycle) and opening of cb1	9
	4. Opening of cb4 the condition of islanding of DG1.	9
Non-Islanding	5. PCC LV-bus load (L1) switching off by opening of cb2.	9
	6. Sudden decrease of the loading on the DG1 (L2) by 40%.	9
	7. Opening of cb8.	9
	8. PCC LV-bus capacitor switching.	9
	9. Three-phase fault on the HV bus (in 5 cycles) with instantaneous and delayed fault-clearing times.	9
	10. PCC LV-bus load (L1) switching on by closing of cb2.	9

4.2 Data Generation

In order to prepare data, which is required to train and test the proposed intelligent model, we simulated 10 sets of pre-defined islanding and non-islanding events. We summarized these events in Table 1. The first four and the second six events are islanding and non-islanding conditions, respectively. To consider different operating conditions for the typical system, the paper [26] defines three operating points for the connected power system and DGs, separately. The three system loadings for the connected power system are normal, minimum maximum. Similar to the connected power system, the operating points, which this paper considered for DGs, are normal, minimum, and maximum load at the PCC-bus. Therefore, the possible combinations of operating points of the connected power system and DGs are nine. These combinations are as follows:

- •The connected power system with normal loading ($Z_s = 0.02$ pu) and PCC-bus normal loading (0.5 + j0.175 pu),
- The connected power system with normal loading ($Z_s = 0.02$ pu) and PCC-bus Min. loading (0.3 + j0.105 pu)
- The connected power system with normal loading ($Z_s = 0.02$ pu) and PCC-bus Max. loading (0.625 + j0.22 pu)

- The connected power system with Min. loading ($Z_s = 0.05$ pu) and PCC-bus normal loading (0.5 + j0.175 pu)
- The connected power system with Min. loading ($Z_s = 0.05$ pu) and PCC-bus Min. loading (0.3 + j0.105 pu)
- The connected power system with Min. loading ($Z_s = 0.05$ pu) and PCC-bus Max. loading (0.625 + j0.22 pu)
- The connected power system with Max. loading ($Z_s = 0.01$ pu) and PCC-bus normal loading (0.5 + j0.175 pu)
- The connected power system with Max. loading ($Z_s = 0.01$ pu) and PCC-bus Min. loading (0.3+j0.105 pu)
- The connected power system with Max. loading ($Z_s = 0.01$ pu) and PCC-bus Max. loading (0.625 + j0.22 pu).

where Z_s is the Thevenin impedance of the connected power system.

In this paper, we simulated each set of events in Table 1 under different above-mentioned operating conditions. Thereby, the total number of the studied events is 90 (10 sets * nine operating conditions), 36 and 54 events for islanding and non-islanding events, respectively.

Generally, when the power mismatch inside an

islanding is small, islanding detection is more difficult. In this paper, we have seen this issue of power mismatch. Specifically, the data cases which we prepared under opening of cb1 (set1 and set3 events) and PCC-bus minimum loading (0.3 + j0.105 pu) have small active and reactive powers mismatch around 5% and 4%, respectively. Under these conditions, just before the islanding situation, the total active power generated by the DG1 and DG2 is 20 MW and the total load of the system is 21 MW i.e. L1 (6 MW) +L2 (5 MW) +L3 (5 MW) +L4 (5 MW).

The proposed RNMG based algorithm needs a data acquisition module for all three-phase voltages and currents. To select a sampling rate for the data acquisition module, the authors considered two important issues. The first one was to satisfy the requirements for an acceptable accuracy of the proposed algorithm. Another one was implementing the proposed algorithm with advanced digital relays. Considering these issues, we selected a sampling frequency equal to 12 kHz in this study. Selecting this sampling rate, we designed a scheme, which has acceptable accuracy and is easy to implement.

Considering the aforementioned scenarios, we have done a wide range of simulations, in each of which we have computed and saved the following system parameters at the PCC bus:
1. Frequency
2. Active power
3. Reactive power
4. Power factor
5. Phase of current zero-sequence
6. Phase of current negative sequence
7. Phase of current positive sequence
8. Current total harmonic distortion (THDi)
9. Magnitude of current zero-sequence
10. Magnitude of current negative sequence
11. Magnitude of current positive sequence
12. Phase of voltage zero-sequence
13. Phase of voltage negative sequence
14. Phase of voltage positive sequence
15. Voltage total harmonic distortion (THDv)
16. Magnitude of voltage zero-sequence
17. Magnitude of voltage negative sequence
18. Magnitude of voltage positive sequence

4.3 Feature Extraction

In this step, the time series of the system parameters within the data window were processed first by the RNMG tool. Then, the energy, standard deviation, and maximum of the RNMG output were calculated as the spatial features of the processed system parameters. This task was repeated for each of system parameters described in Section 4.2, as shown in Fig. 3. Thereby, 54 features were generated for each simulated event. For simplicity, these features were named F1, F2, … and F54. In order to prevent any numerical instabilities,

the generated features were normalized.

4.4 Feature Selection

To select the best features, the procedure shown in Fig. 4 has been proposed. As shown in Fig. 4, the feature selection procedure started first with an empty set of features Y_0. Then, the best feature was selected using the maximum SI described in Section 2.2. The larger the separability measure, the more effective the feature. Subsequently, the first selected feature was removed from the candidate feature set and the next best feature was selected of the remainder of the features. In this procedure, variable t was applied to control the number of the selected features. For the system shown in Fig. 2, the best results were obtained for the best five features ($t = 5$). These features are standard deviation of phase of voltage positive sequence (F41), maximum of phase of voltage positive sequence (F42), maximum of magnitude of voltage positive sequence (F54), standard deviation of frequency (F2), maximum of frequency (F3).

4.5 SVM Classifier Design

In order to design an intelligent scheme, the SVM algorithm was applied. In other words, the optimization problem expressed in Section 2.3 was solved using the generated training data. In this paper, according to the
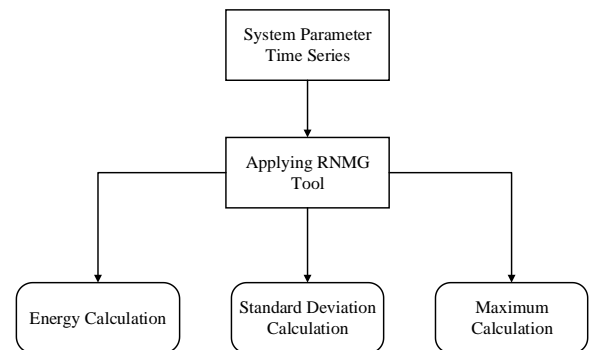

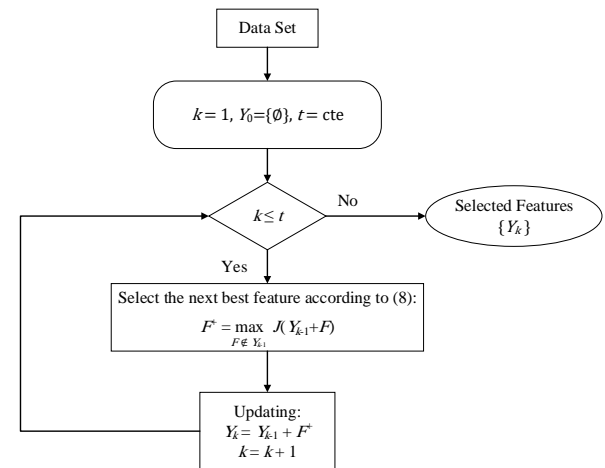**Fig. 3** Proposed feature generation module.

Fig. 4 Proposed feature selection module.

achieved results (Table 4) the hugely popular RBF kernel was selected to handle the islanding detection problem. The penalty factor *C* and the kernel parameter *γ* were determined through a grid search [27] and *k*-fold cross-validation methods. In this paper, a 2-fold cross-validation was used; therefore, one set was used as the training set while the other as the testing set and the process was repeated two times and the average accuracy was calculated for the classifier. The optimum set of these parameters with the final results are shown in Table 2, demonstrating the proposed scheme.

5 Simulation Results and Discussion

In order to investigate the proposed scheme, four tasks were carried out as the following:
1. The comparative assessment of the proposed scheme with some traditional passive methods,
2. The performance analysis of the proposed scheme with different kernel functions,
3. The performance analysis of the proposed scheme with different classifiers,
4. The effect of noise on the performance of the proposed scheme.

Firstly, the system parameters introduced in Section 4.2 were analyzed using the RNMG tool after the islanding initiation. Then, the energy, standard deviation, and maximum of the RNMG output were separately calculated for each parameter. Five superior features were selected according to the procedure in Section 4.4. These features were related to the three system parameters including frequency, the phase of voltage positive sequence, and the magnitude of voltage positive sequence.

The RNMG value for the magnitude of voltage positive sequence in an islanding condition of DGs under the mismatches of $\Delta P = 5.76\%$ and $\Delta Q = 4.01\%$ is shown in Fig. 5. As observed in this figure, the islanding occurred at the time equal to 2s. In this case, 32.7 ms next to islanding initiation, the trip signal was issued. It is necessary to note that the proposed algorithm has a fixed response time, which consists of the time interval of the required data window equal to 16.7 ms, and the time being necessary to islanding judgment. In this paper, we computed the latter based on a 32-bit personal computer with a 3 GHz central processing unit and 4 GB random access memory.

In order to examine the discrimination power of each of the five superior features, the scatter plots shown in Fig. 6 were provided. It can be concluded that the selected features are appropriate for the discrimination of the islanding cases from the non-islanding cases.

Table 2 Characteristics of the selected classifier.

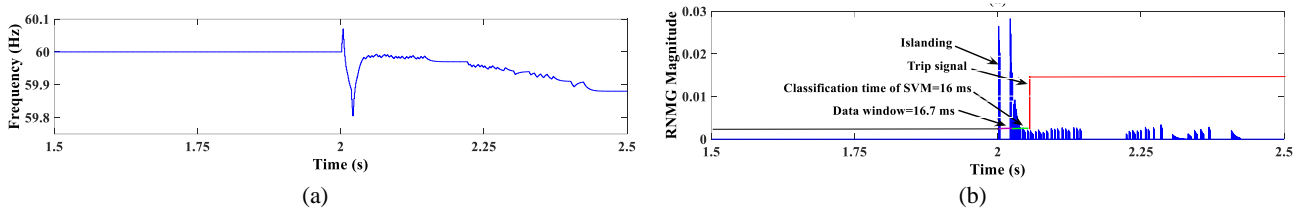|	
Penalty factor (*C*)	26
Kernel parameter (*γ*)	0.28
Number of SVs	14
Selected features	F41, F42, F54, F2, F3
Number of training data	54
Number of testing data	36
2-fold Cross validation accuracy on training data set [%]	96.29
Accuracy on testing data set [%]	100

Fig. 5 a) Frequency and b) RNMG magnitude (under the mismatches of $\Delta P = 5.76\%$ and $\Delta Q = 4.01\%$).
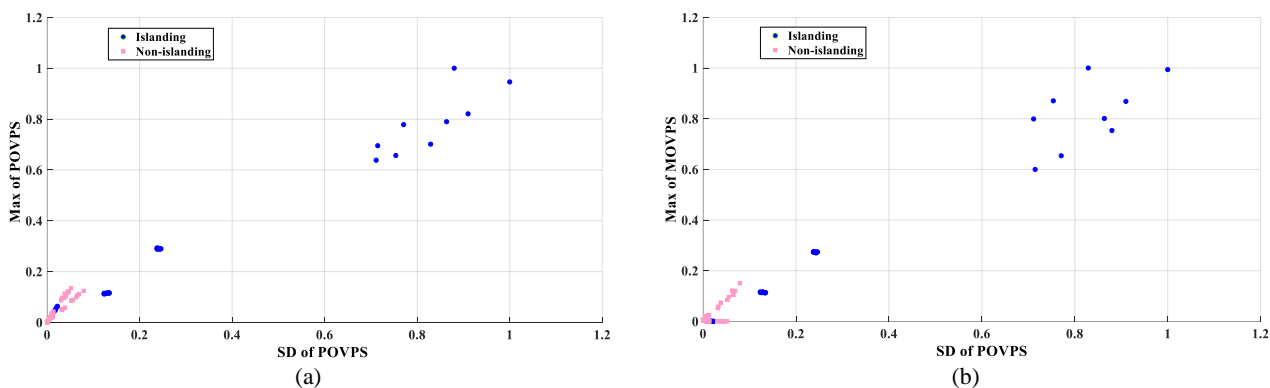

Fig. 6 Scatter plots of features for 90 events. Symbols are: Max (maximum), SD (standard deviation), POVPS (phase of voltage positive sequence), and MOVPS (magnitude of voltage positive sequence).

5.1 Comparative Assessment of the Proposed Scheme with Existing Traditional Methods

In this section, we compared the accuracy and response time of the proposed algorithm with the previous ones, which authors of [29, 31, 32] have reported. These methods are traditional passive methods including over/under voltage (OVP/UVP) [31], over/under frequency (OFP/UFP) [31], rate of change of frequency (ROCOF) [32] and rate of change of power (ROCOP) [29]. To do this comparison, we considered the same data, which was prepared in this paper. In addition, we selected the thresholds for methods in [29] and [31]-[32] based on instructions that were given in related papers and IEEE std. 1547 [3].

The authors summarize the comparative results in Table 3. As observed, the proposed algorithm is superior to the other methods in [31-33], the view point of accuracy. The proposed algorithm has an accuracy of 100%, in contrast to other methods, which do not have acceptable accuracy. The accuracies of OVP/UVP [31], OFP/UFP [31], ROCOF [32] and ROCOP [29] are 58.33%, 88.88%, 86.11% and 83.33%, respectively.

Another index, which is important, is response time. The proposed algorithm has a fixed response time i.e. 32.7 ms. Besides, the response time of other methods is variable and the maximum response time of OVP/UVP [31], OFP/UFP [31], ROCOF [32], and ROCOP [29] are 4 ms, 1792 ms, 20.8 ms, and 20.5 ms, respectively. Therefore, the viewpoint of response time, other methods with the exception of OFP/UFP [31] are more rapid than the proposed algorithm. However, as mentioned above, none of them have acceptable accuracy to judge whether a situation is islanding or not. In other words, the accuracy of the proposed algorithm is excellent and whose response time is much smaller than the maximum delay of 2 s that the IEEE std. 1547 [3] emphasizes to detect islanding and to disconnect all DGs from the distribution system. Thereby, we can conclude that the proposed method is more appropriate to the previous ones [29, 31, 32] to detect an islanding situation.

As an example, Fig. 7 shows the performance of methods including OVP/UVP [31], OFP/UFP [31], ROCOF [32] and ROCOP [29] during an islanding

Table 3 Performance of islanding detection methods.

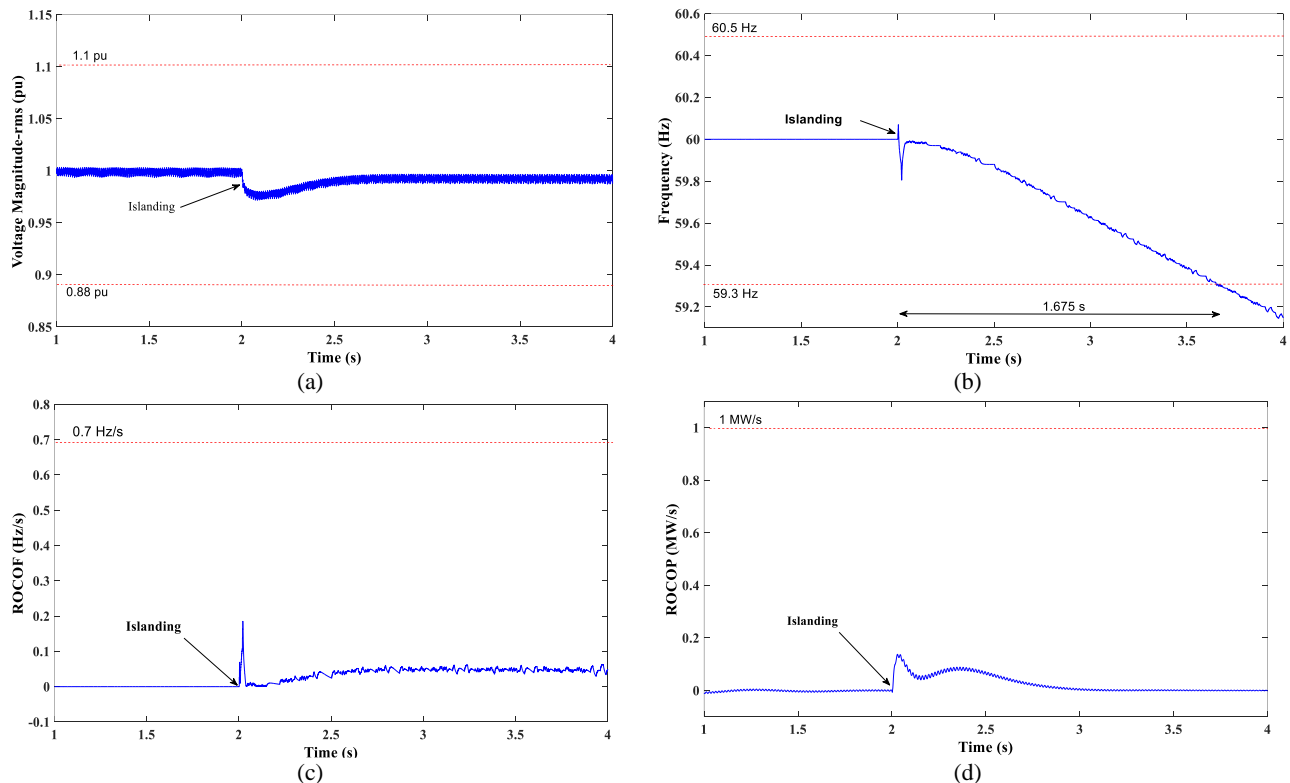| Method	Model	Accuracy on testing data set [%]	Response time [ms]	
This paper	Intelligent	100	Fixed	32.7
OVP/UVP [31]	Traditional	58.33	Variable-Max response time	4
OFP/UFP [31]	Traditional	88.88	Variable-Max response time	1792
ROCOF [32]	Traditional	86.11	Variable-Max response time	20.8
ROCOP [29]	Traditional	83.33	Variable-Max response time	20.5

Fig. 7 Performance of a) OVP/UVP, b) OFP/UFP c) ROCOF, and d) ROCOP during an islanding condition under the mismatches of $\Delta P = 5.76\%$ and $\Delta Q = 4.01\%$

condition under the mismatches of $\Delta P = 5.76\%$ and $\Delta Q = 4.01\%$. As observed in Fig. 7(a), The UVP/OVP [31] method is unable to detect this condition because the magnitude of voltage is lower than the threshold value. According to Fig. 7(b), the UFP/OFP [31] method detects the islanding condition within a long time 1.675 s. As shown in Fig. 7(c), the ROCOF method [32] is unable to detect this condition because the df/dt is not more than the threshold value of 0.7 Hz/s. In Fig. 7(d), the amount of dP/dt does not become more than the threshold value of 1 MW/s, that is why ROCOP [29] is not able to detect the islanding condition. It is worthy to note that the proposed algorithm, as shown in Fig. 5, is able to detect this islanding condition within 32.7 ms.

5.2 Effect of Noise

In practical conditions, noises, which come from several different types of sources, contaminate the measurements. Therefore, it is necessary to evaluate the proposed scheme in such conditions. In order to examine the performance of the proposed scheme on the noisy testing data set, at first, we trained the SVM classifier by the clean training data set, and then, obtained the prediction accuracy of the trained classifier on the noisy testing data set. Fig. 8 shows the prediction accuracy of the proposed scheme. As observed, the accuracy for signal to noise ratios (SNRs) including 60 dB, 50 dB and 40 dB is 100% and for 30 dB is 94.44%. Therefore, the proposed algorithm has an acceptable accuracy for SNRs higher than 30 dB. However, for SNRs smaller than 30 dB, the prediction accuracy is degraded. Thereby, in substations with SNRs smaller than 30 dB, we highly recommend using an anti-aliasing filter.

5.3 Kernel Type Selection

In order to demonstrate the RBF kernel for detecting islanding and non-islanding conditions, it was necessary to apply other kernel functions in the classifier of the proposed scheme. First, we applied the clean data to separately train the SVM classifier with polynomial,
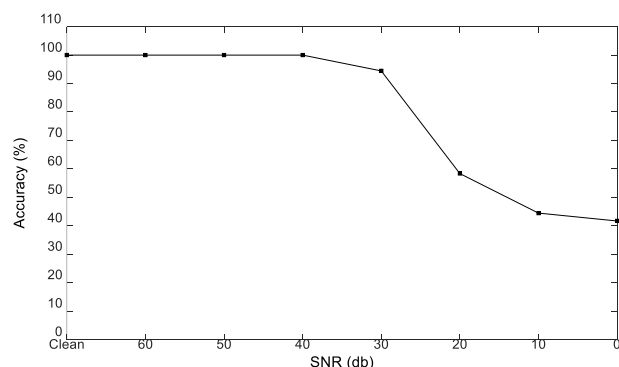
MLP, and linear as kernel functions, and then, obtained the prediction accuracy results based on clean and noisy testing data set. Table 4 shows the results are. According to clean testing data, the proposed algorithm with RBF as kernel function has an accuracy of 100%, in contrast to other kernels. The accuracies of the proposed algorithm with polynomial, MLP, and linear as kernel functions are 97.22%, 97.22%, and 94.44%, respectively. It is clear that the RBF is superior to other kernel functions including polynomial, MLP, and linear. As observed in the table, we can conclude the same result for noisy testing data. Thereby, we recommend using RBF as the kernel function in the proposed algorithm.

5.4 Classifier Type Selection

In order to discuss the necessity of selecting an appropriate classifier type, we the decision function module of the proposed algorithm by the k-nearest neighbor (k-NN) classifier [23, 24], in addition to the SVM classifier. Moreover, we determined the neighbor number in the k-NN classifier by the grid search method mentioned in Section 4.5. Table 5 shows the results of the SVM and k-NN classifiers based on clean and noisy testing data sets. As an observer, both classifiers have excellent accuracy on clean data set. However, the accuracy of k-NN decreases to 94.44% and 91.66% for noisy data set with SNRs equal to 40 dB and 30 dB, respectively. In contrast, the proposed algorithm with the SVM classifier, the accuracy only for noisy data set equal to 30 dB decreases to 94.44%. Thereby, we can conclude that the SVM classifier is superior to k-NN, the viewpoint of noisy data set.

6 Conclusion

The authors have proposed to use a new digital filter based on mathematical morphology (MM) to design a scheme to detect an islanding situation. The learning algorithm, which we used to prepare the scheme, is the support vector machine (SVM) with radial basis function (RBF) as a kernel. The employed digital filter

Fig. 8 Prediction accuracy values of the clean and noisy testing data set of the trained SVM classifier.

Table 4 Kernel type selection results.

Kernel	Prediction accuracy on testing data set [%]				
	Clean	SNR [dB]			
		60	50	40	30
RBF	100	100	100	100	94.44
Polynomial	97.22	97.22	97.22	94.44	86.11
MLP	97.22	97.22	91.66	88.88	83.33
Linear	94.44	94.44	91.66	86.11	83.33

Table 5 Classifier type selection results.

Classifier type	Prediction accuracy on testing data set [%]				
	clean	SNR [dB]			
		60	50	40	30
SVM	100	100	100	100	94.44
k-NN	100	100	100	94.44	91.66

is reduced-noise morphological gradient (RNMG). Most notably, this is the first study to our knowledge to take advantage of RNMG to detect islanding detection. One of the main characteristics is that it can highlight irregularities of the time series under analysis. Another advantage of this special digital filter is to being robust under noisy conditions. The authors examined and reported the robustness of the RNMG based proposed scheme under conditions with SNRs higher than 30 dB. In addition, the authors employed the separability index (SI) to show that among the system parameters, the RNMG magnitude of the frequency, the phase of voltage positive sequence, and the magnitude of voltage positive sequence have the highest discrimination power between islanding and non-islanding cases. Besides, the obtained results from the case study show that the proposed scheme can detect islanding conditions within 32.7 ms and is more appropriate than other traditional methods including OVP/UVP, OFP/UFP, ROCOF, and ROCOP.

Appendix

This appendix contains the data required for the application example shown in Fig. 2. The base power has been chosen as 20 MVA [26].

1) Generators data:
   - Equivalent system G:
       rated short-circuit MVA = 1000, f = 60 Hz, rated kV = 69, V_{base} = 69 kV.
   - Generators DG1 and DG2:
       rated MVA= 10, f = 60 Hz, 54 poles, Yn, rated kV = 13.8, V_{base} = 13.8 kV, Inertia constant H = 3.0 sec., R_0 = 0.0025 pu, X_0 = 0.113 pu, R_1 = 0.001 pu, X_1 = 0.15 pu, X_d = 1.028 pu, X_q = 0.654 pu, X'_d = 0.34 pu, X'_q = 0.654 pu, X''_d = 0.253 pu, X''_q = 0.298 pu, T'_{d0} = 7.5 s, T'_{q0} = 0 s, T''_{d0} = 0.07 s, T''_{q0} = 0.09 s.

2) Power transformer data:
   - Transformer T1:
       rated MVA = 25, f = 60 Hz, Rated kV = 69/13.8, Dyn1, V_{base} = 13.8 kV, R_1 = 0.00375 pu, X_1 = 0.1 pu, R_m = 500 pu, X_m = 500 pu.
   - Transformer T2 and T3:
       rated MVA = 10, f = 60 Hz, rated kV = 13.8/13.8, Ynd1, V_{base} = 13.8 kV, R_1 = 0.00375 pu, X_1 = 0.1 pu, R_m = 500 pu, X_m = 500 pu.

3) Transmission lines data:
       Rated kV = 13.8, rated MVA = 20, V_{base} = 13.8 kV, R_{0L} = 0.0414 Ω/km, R_{1L} = 0.0138 Ω/km, X_{0L} = 0.0534 Ω/km, X_{1L} = 0.0178 Ω/km, X_{0CL} = 5.1 nF/km, X_{1CL} = 17 nF/km, Line1 = 20 km, Line2 = 10 km, Line3 = 10 km.

4) Normal loading data: (Rated kV=13.8)

L1 = 10 MW, 3.5 MVA
L2 = 5.0 MW, 2.0 MVAR
L3 = 5.0 MW, 2.0 MVAR
L4 = 5.0 MW, 2.0 MVAR.

References

[1] IEEE Power System Relaying Committee WG D3 Workgroup, "IEEE PSRC report, Impact of distributed resources on distribution line protection," 2004.

[2] A. Khamis, H. Shareef, E. Bizkevelci, and T. Khatib, "A review of islanding detection techniques for renewable distributed generation systems," R*enewable and Sustainable Energy Reviews*, Vol. 28, pp. 483–493, 2013.

[3] IEEE Application Guide for IEEE Std 1547(TM), "IEEE standard for interconnecting distributed resources with electric power systems," in *IEEE Std 1547.2-2008*, pp.1–217, Apr. 2009.

[4] W. Xu, G. Zhang, C. Li, W. Wang, G. Wang, and J. Kliber, "A power line signaling based technique for anti-islanding protection of distributed generators—Part I: Scheme and analysis," *IEEE Transactions on Power Delivery*, Vol. 22, No. 3, pp. 1758–1766, 2007.

[5] W. Wang, J. Kliber, G. Zhang, W. Xu, B. Howell, and T. Palladino, "A power line signaling based scheme for anti-islanding protection of distributed generators—Part II: Field test results," *IEEE Transactions on Power Delivery*, Vol. 22, No. 3, pp. 1767–1772, 2007.

[6] T. Bei, "Accurate active islanding detection method for grid-tied inverters in distributed generation," *IET Renewable Power Generation*, Vol. 11, No. 13, pp. 1633–1639, 2017.

[7] C. Zhang, Z. Lü, T. Yang, and L. Wang, "A novel islanding detection method based on positive feedback between reactive current and frequency," *Automation of Electric Power Systems*, Vol. 36, No. 1, pp. 193–199, 2012.

[8] L. Lopes and Z. Yongzheng, "Islanding detection assessment of multiinverter systems with active frequency drifting methods," *IEEE Transactions on Power Delivery*, Vol. 23, pp. 480–486, 2008.

[9] J. E. Kim and J. S. Hwang, "Islanding detection method of distributed generation units connected to power distribution system," in *International Conference on Power System Technology. Proceedings (Cat. No. 00EX409)*, Vol. 2, pp. 643–647, 2000.

[10] N. Lidula and A. Rajapakse, "A pattern recognition approach for detecting power islands using transient signals—Part I: Design and implementation," *IEEE Transactions on Power Delivery*, Vol. 25, No. 4, pp. 3070–3077, 2010.

[11] S. R. Mohanty, N. Kishor, P. K. Ray, and J. P. Catalão, "Comparative study of advanced signal processing techniques for islanding detection in a hybrid distributed generation system," *IEEE Transactions on Sustainable Energy*, Vol. 6, No. 1, pp. 122–131, 2015.

[12] P. K. Ray, S. R. Mohanty, and N. Kishor, "Islanding and power quality disturbance detection in grid-connected hybrid power system using wavelet and S-transform," *IEEE Transactions on Smart Grid*, Vol. 3, No. 3, pp. 1082–1094, 2012.

[13] M. A. Farhan and K. S. Swarup, "Mathematical morphology-based islanding detection for distributed generation," *IET Generation, Transmission & Distribution*, Vol. 10, No. 2, pp. 518–525, 2016.

[14] E. A. P. Gomes, J. C. M. Vieira1, D. V. Coury, A. C. B. Delbem, "Islanding detection of synchronous distributed generators using data mining complex correlations," *IET Generation, Transmission & Distribution*, Vol. 12, No. 17, pp. 3935–3942, 2018.

[15] S. Chandak, M. Mishra, S. Nayak, P. K. Rout, "Optimal feature selection for islanding detection in distributed generation," *IET Smart Grid*, Vol. 1, No. 3, pp. 85–95, 2018.

[16] M. R. Alam, K. M. Muttaqi, A. Bouzerdoum, "Evaluating the effectiveness of a machine learning approach based on response time and reliability for islanding detection of distributed generation," *IET Renewable Power Generation*, Vol. 11, No. 11, pp. 1392–1400, 2017.

[17] Q. Cui, K. El-Arroudi, and G. Joós, "Islanding detection of hybrid distributed generation under reduced non-detection zone," *IEEE Transactions on Smart Grid*, Vol. 9, No. 5, pp. 5027–5037, 2018.

[18] H. Vahedi, G. B. Gharehpetian, and M. Karrari, "Application of duffing oscillators for passive islanding detection of inverter-based distributed generation units," *IEEE Transactions on Power Delivery*, Vol. 27, No. 4, pp. 1973–1983, 2012.

[19] M. Harikrishna and J. Premalata, "Phase angle-based PC technique for islanding detection of distributed generations," *IET Renewable Power Generation*, Vol. 12, No. 6, pp. 735–746, 2018.

[20] M. Bakhshi, R. Noroozian, and G. B. Gharehpetian, "Novel islanding detection method for multiple DGs based on forced Helmholtz oscillator," *IEEE Transactions on Smart Grid*, Vol. 9, No. 6, pp. 6448–6460, 2018.

[21] Z. Yu-Qian, G. Wei-Hua, C. Zhen-Cheng, T. Jing-Tian, and L. Ling-Yun, "Medical images edge detection based on mathematical morphology," in *Engineering in Medicine and Biology Society*, pp. 6492–6495, 2006.

[22] Q. H. Wu, Z. Lu, and T. Ji, *Protective relaying of power systems using mathematical morphology*. Springer Science & Business Media, 2009.

[23] S. Theodoridis and K. Koutroumbas, *Pattern recognition*. Elsevier Academic Press, 2nd ed., 2000.

[24] K. Fukunaga, *Introduction to statistical pattern recognition*. Morgan Kaufinann, 2nd ed., 1990.

[25] C. Corte and V. Vapnik, "Support-vector networks," *Machine Learning*, Vol. 20, No. 3, pp. 273–297, 1995.

[26] K. El-Arroudi, G. Joós, I. Kamwa, and D. T. McGillis, "Intelligent-based approach to islanding detection in distributed generation," *IEEE Transactions on Power Delivery*, Vol. 22, No. 2, pp. 828–835, 2007.

[27] C. W. Hsu, C. C. Chang, and C. J. Lin, "A practical guide to support vector classification," [Online]. Available: http://www.csie.ntu.edu.tw/~cjlin/talks/freiburg.pdf.

[28] V. Jose, W. Freitas, W. Xu, and A. Morelato, "Efficient coordination of ROCOF and frequency relays for distributed generation protection by using the application region," *IEEE Transactions on Power Delivery*, Vol. 12, No. 4, pp. 1878–1884, 2006.

[29] M. Redfern, O. Usta, and G. Fielding, "Protection against loss of utility grid supply for a dispersed storage and generation unit," *IEEE Transactions on Power Delivery*, Vol. 8, No. 3, pp. 948–954, 1993.

[30] X. Wu and V. Kumar, *The top ten algorithms in data mining*. CRC Press, 2009.

[31] H. H. Zeineldin and J. L. Kirtley, "A simple technique for islanding detection with negligible nondetection zone," *IEEE Transactions on Power Delivery*, Vol. 24, No. 2, pp. 779–786, Apr. 2009.

[32] J. C. Vieira, W. Freitas, Z. Huang, W. Xu, and A. Morelato, "Formulas for predicting the dynamic performance of ROCOF relays for embedded generation applications," *IEE Proceedings-Generation, Transmission and Distribution*, Vol. 153, No. 4, pp. 399–406, 2006.

[33] M. Suman and V. Murali, "Hybrid analyzing technique based active islanding detection for multiple DGs," *IEEE Transactions on Industrial Informatics*, Vol. 5, No. 3, pp. 1311–1320, 2018.

[34] A. Rostami, A. Jalilian, S. Zabihi, J. Olamaei, and E. Pouresmaeil, "Islanding detection of distributed generation based on parallel inductive impedance switching," *IEEE Systems Journal*, Vol. 14, No. 1, pp. 813–823, 2019.

[35] M. R. Alam, M. T. A. Begum, and K. M. Muttaqi, "Assessing the performance of ROCOF relay for anti-islanding protection of distributed generation under subcritical region of power imbalance," *IEEE Transactions on Industry Applications*, Vol. 55, No. 5, pp. 5395–5405, 2019.

[36] N. Ruchita, M. Biswal, and N. Kishor, "A transient component based approach for islanding detection in distributed generation," *IEEE Transactions on Sustainable Energy*, Vol. 10, No. 3, pp. 1129–1138, 2019.

[37] M. R. Alam, M. T. A. Begum, and B. Mather, "Islanding detection of distributed generation using electrical variables in space vector domain," *IEEE Transactions on Power Delivery*, Vol. 35, No. 2, pp. 861–870, 2019.

S. Shadpey was born in Iran. He received the B.Sc. degree in Electrical Engineering from Shahid Beheshti University (SBU), Tehran, Iran and the M.Sc. degree in Electrical Engineering from the Jundi-Shapour University of Technology, Dezfoul, Iran, respectively. His research interests include the application of pattern-recognition methods in digital power system protection and power system studies.

M. Sarlak was born in Andimeshk, Iran, in 1981. He received the B.Sc. degree in Electrical Engineering from Khajeh Nasir Toosi University of Technology (KNTU), Tehran, Iran, in 2003 and the M.Sc. and Ph.D. degrees in Electrical Engineering from Iran University of Science and Technology, Tehran (IUST), Iran, in 2005 and 2011, respectively. Currently, he is an Assistant Professor in the Electrical and Computer Engineering Department, Jundi-Shapour University of Technology, Dezfoul. His research interests include the application of pattern-recognition methods in digital power system protection and power system studies.